Modulated induction thermal plasmas - Fundamentals and applications

doi: 10.1002/tee.20432

Review Paper

Modulated Induction Thermal Plasmas – Fundamentals and Applications –

Yasunori Tanaka* Member
Yoshihiko Uesugi* Member

This paper reviews fundamentals and applications of modulated induction thermal plasmas that have been developed. The coil current modulation of the order of several hundreds amperes allows one to make a large disturbance in high-pressure and high temperature plasmas, and also to control the temperature and radical density in thermal plasmas in time domain. Examples will be introduced on application of the modulated induction thermal plasma to surface modification, in which thermally and chemically non-equilibrium effects are essential in temperature and radical density fields. Finally, dynamic behaviors of an arbitrary-waveform modulated induction thermal plasma that has recently been developed were also introduced as a new type of modulated induction thermal plasmas.

Keywords: Thermal Plasma, Modulation, Ar Excitation Temperature, Non-Equilibrium Effects

1. Introduction

The inductively coupled thermal plasma (ICTP) is widely used for various material processings like synthesis of nanopowder, thermal barrier coatings, diamond film deposition and surface modification etc [(1)–(9)]. One advantage of the thermal plasma is to have much higher densities of reactive species or radicals, and high gas temperature. However, gas temperature in thermal plasmas is sometimes too high and is difficult to control. In order to control gas temperature and densities of reactive atoms/molecules in thermal plasmas, we have developed a system of several-tens kW-class pulse-modulated induction thermal plasma (PMITP) [(10)–(17)]. This system can modulate the amplitude of the coil current sustaining induction thermal plasmas in a rectangular waveform in milliseconds. The millisecond rectangular modulation in the coil current remarkably perturbs the temperature of thermal plasmas and it can markedly change densities of atoms/molecules in thermal plasmas. Through this periodical perturbation on the thermal plasmas, we can then control the time-averaged value of them in time domain [(16) (17)]. This modulation also provides non-equilibrium effects even in high-pressure thermal plasmas. On the other hand, some studies have been continued for application of the PMITP to materials processings [(18)–(23)]. For example, Ohashi et al. applied the Ar-H_2 PMITP for hydrogen doping to ZnO and found that H atoms can be implanted into ZnO by treatment with an Ar-H_2 PMITP, thereby improving its photoluminescence [(19) (20)]. We have also investigated to apply the Ar-N_2 PMITP for surface nitridation processing of materials [(21)–(23)].

This paper reviews fundamentals and applications of modulated induction thermal plasmas that we have developed. First of all, the system of pulse-modulated induction thermal plasmas is described. Secondly, fundamental dynamic behaviors of PMITP are introduced, which have been obtained mainly in our experiments. The experimental results indicated that the millisecond rectangular modulation in the coil current provides a large disturbance in the radiation intensity of the Ar line and also that the modulation can change the Ar excitation temperature from 5000 to 10000 K especially in Ar-CO_2 PMITP [(16)]. Thirdly, an example is shown in applications of modulated induction thermal plasmas for high-speed surface nitridation processings. In this work, we have found that the rectangular modulation of the coil current can provide the increased number of excited N atom and at the same time the decreased enthalpy flow onto the specimen irradiated by Ar-N_2 PMITP. Both the nitrogen atomic density and the enthalpy flow are crucial for nitridation processing using thermal plasmas. On the other hand, our non-equilibrium calculations imply that the above simultaneous control of the increased nitrogen atomic density and the decreased enthalpy flow is due to chemically non-equilibrium effects [(23)–(26)]. Some other applications of PMITP to surface modification will be introduced briefly [(18)–(20)]. Finally, a new type of modulated induction thermal plasmas, i.e. the arbitrary waveform modulated induction thermal plasma (AMITP) is introduced, and the time evolution in Ar excitation temperature in Ar AMITP is described [(27)]. This system can modulate the amplitude of the coil current to follow a control signal formed in not only a rectangular waveform but also an externally-given arbitrary waveform. Such a modulation of the coil current makes the detailed control possible in the temperature of thermal plasmas.

* Division of Electrical Engineering & Computer Science, Kanazawa University, Kakuma, Kanazawa 920-1192, Japan

Table 1. Characteristic times in cm-class thermal plasmas at 5000 K at atmospheric pressure

Phenomena	Characteristic time
Thermal conduction	$\sim 10^{-4}$–10^{-2} s
Diffusion	$\sim 10^{-4}$–10^{-3} s
Convection	$\sim 10^{-4}$–10^{-3} s
Reactions	$\sim 10^{-7}$–10^{-2} s

2. Characteristic times in thermal plasmas

It is important to understand characteristic times for changing the state in thermal plasmas. Let us consider characteristic times in centimeter-class Ar thermal plasmas around 5000 K at atmospheric pressure. The typical characteristic times for thermal conduction, diffusion and convection were estimated by the following simple equations:

$$t_{\mathrm{cond}} = \frac{\rho C_{\mathrm{p}}}{\lambda} L^2 \quad \cdots\cdots (1)$$

$$t_{\mathrm{diff}} = \frac{L^2}{D} \quad \cdots\cdots (2)$$

$$t_{\mathrm{conv}} = \frac{L}{u} \quad \cdots\cdots (3)$$

$$t_{\mathrm{reac}} = \frac{1}{\alpha n} \quad \cdots\cdots (4)$$

where t_{cond}, t_{diff}, t_{conv}, and t_{cond} are respectively the characteristic times for thermal conduction, diffusion, convection and reactions, L is the characteristic length, ρ is the mass density, C_{p} is the specific heat, λ is the thermal conductivity, D is the diffusion coefficient, u is the gas velocity, α is the reaction rate, n is the number density of the plasma. In this estimation, u of 10–100 m/s was used for induction thermal plasmas [26].

According to Tab. 1, thermal conduction, diffusion and convection have characteristic times of several milliseconds. Reactions have wide time range because various type of reactions including ionization, recombination and excitation are present in thermal plasmas. On the other hand, the radio-frequency (rf) cycle time of the coil current is about 10^{-7}–10^{-5} s since the frequency of 0.1–10 MHz is usually adopted for the coil current sustaining high-pressure thermal plasmas. This rf cycle time is much shorter than the above characteristic times except reactions, which means that plasma is statically established without any disturbance in macroscopic sight by such an rf coil current. Meanwhile, modulation cycle time used for modulated thermal plasmas is of the order of milli-seconds. This modulation cycle in milliseconds has a similar order to the characteristic times in thermal plasmas. Therefore, such a millisecond modulation of the coil current can markedly perturb even the heavy-particle temperature and gas flow fields as well as reaction fields. In addition, controlling the modulation amplitude of the coil current and the modulation waveform etc. enables us to control the temperature and gas flow fields in time domain.

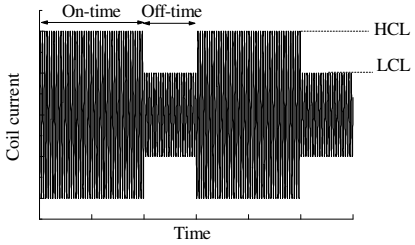

Fig. 1. Pulse modulated coil current.

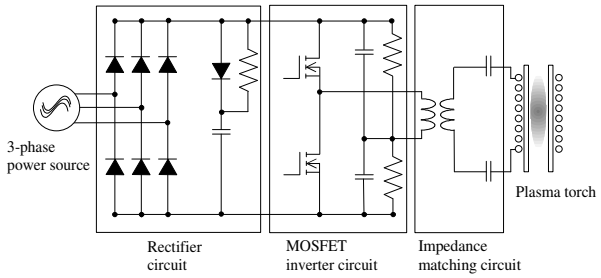

Fig. 2. Electric circuit for PMITP [16] [17].

3. Fundamentals of pulse modulated induction thermal plasmas (PMITP)

3.1 Modulation of coil current for PMITP

For sustaining the pulse modulated induction thermal plasma (PMITP), the coil current modulated in a rectangular waveform shown in Fig. 1 was actually used. This modulation of the coil current in milliseconds markedly perturbs thermal plasmas, then the heavy particle temperature of plasmas changes periodically as described in the previous section. Setting several modulation parameters such as the higher current level (HCL), the lower current level (LCL), and on-time, and off-time as indicated in Fig. 1 and a shimmer current level (LCL/HCL) makes it possible to control the time-averaged temperature of thermal plasmas.

3.2 Electric circuit and plasma torch To realize a PMITP system, we have used a high-power semiconductor inverter power supply. Fig. 2 depicts the electric circuit of a power supply for PMITP. The system mainly contains four components: a rectifier circuit, an inverter circuit, an impedance-matching circuit and an ICP torch. The details of this power supply can be found in [16] [17]. The coil current amplitude is modulated by controlling fire angle of MOSFET elements intentionally to shift from the impedance matching point.

Fig. 3 illustrates a configuration of a plasma torch for PMITP. The plasma torch is composed of two coaxial quartz tubes with a 330 mm length. The inner tube has an inside diameter of 70 mm. Between these two tubes, cooling water flows to keep the temperature of the tube wall to be 300 K. This plasma torch has an eight-turn induction coil around the quartz tube. Downstream of the plasma torch, a water-cooled reaction chamber is installed. Argon and other gas mixtures are supplied as a sheath gas along the inside wall of the inside quartz

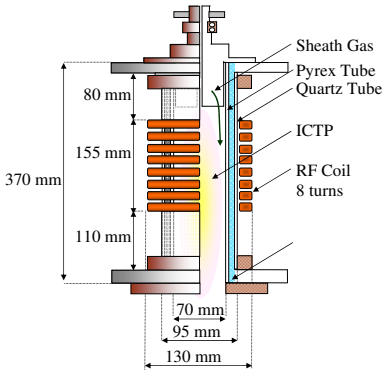

Fig. 3. Schematic diagram of plasma torch.

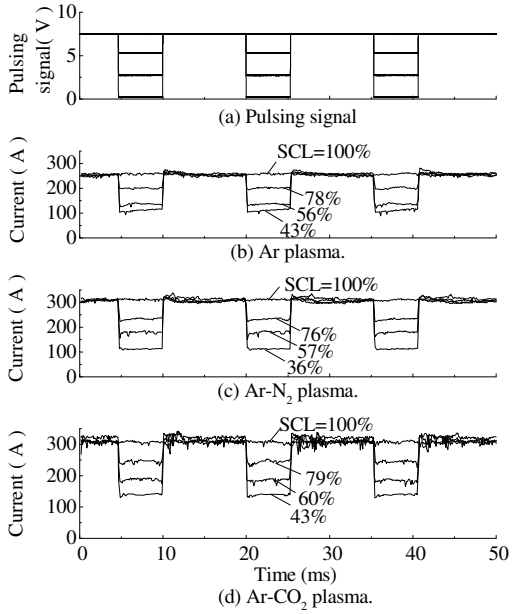

Fig. 4. Coil current waveform for different PMITPs [16] [17].

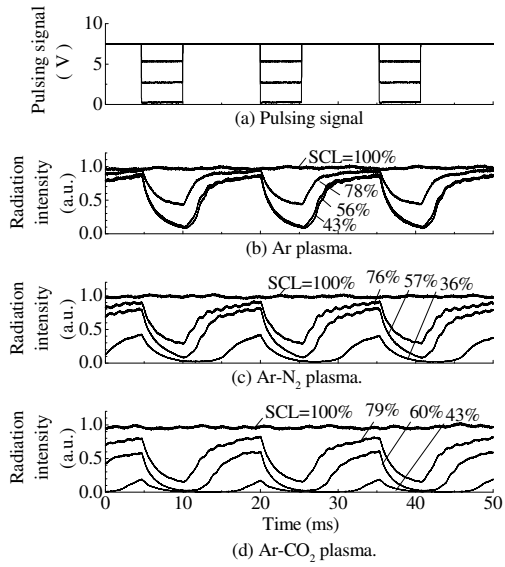

Fig. 5. Time evolution in radiation intensity of Ar line at 751 nm from different PMITPs [16] [17].

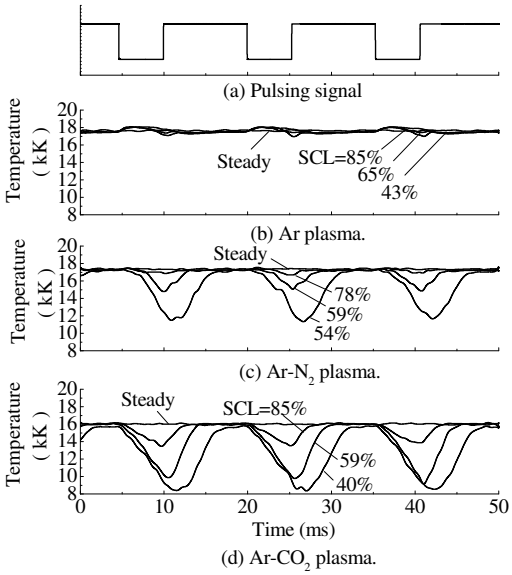

Fig. 6. Time variation in Ar excitation temperature in different PMITP [16] [17].

tube. The dynamic behavior of thermal plasma depends on the configuration and the scale of a plasma torch.

3.3 Fundamental dynamic behaviors of PMITP

Fundamental dynamic behavior is a basic data to know the nature of PMITP. Fig. 4 (a) indicates pulse control signal, (b) is the coil current amplitude for Ar PMITP. (c) is the coil current amplitude for Ar-N_2 PMITP, (d) is the coil current amplitude for Ar-CO_2 PMITP [16] [17]. The shimmer current level (SCL=LCL/HCL) is taken as a parameter. For any gas mixture cases, the coil current amplitude can be changed in 80 μs during its rapid increase and its rapid decrease. Consequently, the inherent characteristic times of thermal plasmas with different gas mixtures can be estimated using this PMITP system, because the inherent characteristic times are much longer than the above time for rapid increase in the current amplitude.

Here are introduced some examples of dynamic behaviors of Ar PMITP with or without molecular gases. Fig. 5 indicates the time evolution in radiation intensity of Ar atomic line at 751 nm for different SCL [16] [17]. The input power is 30 kW for 100%SCL, i.e. for non-modulation operation, and the pressure is atmospheric pressure in the torch. Ar gas flow rate is 100 slpm, and additional gas flow rate is 2.5 slpm. The radiation intensity of the Ar line was measured at 10 mm below the coil end. As seen in this figure, the radiation intensity can be modulated following the modulated coil current. This change in the radiation intensity means that the number of Ar excited atom in the PMITP changed according to the modulation of the coil current. That response in radiation intensity from Ar-N_2 or Ar-CO_2 PMITP is slower than that from Ar PMITP. This difference in response time indicates that addition of molecular gas makes it difficult for Ar thermal plasmas to recover from low temperature state to high temperature state in the PMITP.

Next, time evolution in Ar excitation temperature was

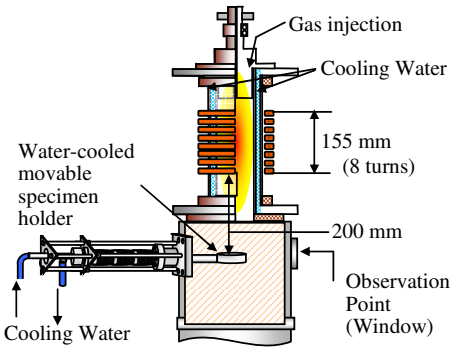

Fig. 7. Specimen position for nitridation processing using PMITP.

estimated to confirm effects of such a coil current modulation in the rectangular waveform on the temperature of thermal plasmas [16] [17]. The input power is 30 kW for 100%SCL, i.e. for non-modulation operation, and the pressure is atmospheric pressure in the torch. Ar gas flow rate is 100 slpm, and additional gas flow rate is 2.5 slpm. The Ar excitation temperature was determined by the two-line method using the net radiation intensities of Ar atomic lines at 703 nm and 714 nm after subtracting continuum components. Fig. 6 indicates (a) the pulse control signal, (b)the time evolution in the Ar excitation temperature for Ar PMITP, (c) that for Ar-N_2 PMITP, (d) that for Ar-CO_2 PMITP. These Ar excitation temperatures were also measured at 10 mm below the coil end. In case of Ar PMITP, Ar excitation temperature is hardly changed by the modulation of the coil current. On the other hand, in molecular gas seeded Ar PMITP, i.e. Ar-N_2 and Ar-CO_2 PMITP, Ar excitation temperature can be changed markedly following the modulated coil current. Particularly, in Ar-CO_2 PMITP, the coil current modulation can change Ar excitation temperature by 2000–8000 K depending on the shimmer current level (SCL).

4. Application of Ar-N_2 PMITP for surface nitridation

It is interesting to apply PMITP with the controlled temperature and radical densities to material processings. Up to now, application of PMITP for surface modification processing has been tried [21] [22]. Here, we introduce nitridation processing of Ti metallic surface using Ar-N_2 PMITP.

4.1 Plasma torch, reaction chamber and specimen position for nitridation processing For nitridation processing, a Ti specimen was installed to be irradiated by Ar-N_2 PMITP downstream of the plasma torch. Fig. 7 shows a schematic diagram of the plasma torch, the reaction chamber and the titanium specimen for nitridation processing. The plasma torch is the same to that in Fig. 3. Downstream of this plasma torch, a water-cooled reaction chamber with a specimen holder is installed. The specimen holder holds a 15-mm-diameter, 5-mm-thick titanium specimen. The specimen was irradiated directly by an Ar-N_2 PMITP. The Ar-N_2 gas mixture was supplied as a sheath gas with a swirl along the interior of the inner quartz tube from the top of the plasma torch. The total gas flow rate was fixed at 100.0 slpm (= l/min). The nitrogen gas flow rate Q_{N_2} was set to a value of 2.0 or 4.0 slpm. Pressure inside the chamber was fixed to 30 kPa (230 torr). The 'on-time' and 'off-time' were set respectively to 10 ms and 5 ms in this experiment. In the present work, we fixed the time-averaged input power to the MOSFET inverter power supply at the same value of 15 kW for any SCL condition. This fixed power control can be realized using a higher HCL and a lower LCL to the current amplitude in the non-modulation condition. This fixed power condition enables us to compare results under the same electric input power cost.

4.2 XRD analysis of the irradiated specimen surface The specimen surface of Ti irradiated by an Ar-N_2 PMITP was analyzed by X-ray diffraction (XRD) to find the effect of the current modulation on the specimen surface composition. Fig. 8 shows examples of XRD spectra for the specimen surface irradiated by Ar-N_2 PMITP. The Ar and N_2 gas flow rates were 98 slpm and 2 slpm, respectively. In this study, we do not use hydrogen to simplify the experimental condition. The irradiation time is 5 min for all case. As seen, XRD spectra for TiN (1 1 1), TiN (1 0 1) and TiN (2 0 0) can be seen in case of SCL=100%, i.e non-modulation case. On the other hand, at SCL=70%, the intensities of TiN (1 1 1) and TiN (2 0 0) decreases while those of TiN (1 0 1) increases and the spectrum of Ti_2N (1 0 1) appears. At further lower SCL, i.e. SCL=40%, the XRD spectra is again similar to that at SCL=100%, although the modulation condition (then the surface temperature) is different. As a result, the influence of the coil-current modulation is clearly apparent in XRD spectra for the irradiated surface even at the same input power and at the same specimen position. It can be emphasized that the coil current modulation effects the surface structure.

4.3 Modulation effect on increased number of nitrogen excited atoms The neutral nitrogen atomic density irradiating the specimen surface is important for surface nitridation processing using thermal plasmas. We measured the radiation intensity of nitrogen atomic line at 746.8 nm to estimate the behavior of the nitrogen atomic density [21] [22]. Fig. 9 shows the time evolution in the radiation intensity of the nitrogen atomic line from the Ar-N_2 PMITP for SCL of 100, 70 and 40%. The nitrogen gas flow rate Q_{N_2} is 4.0 slpm. As seen, the peak value of the radiation intensity increases with reducing SCL. This result indicates that the pulse modulation of the coil current increases the instantaneous density of the excited nitrogen atom in the observation region, i.e. near the specimen surface.

For surface nitridation processing, the time-averaged nitrogen density as well as the instantaneous value is also crucial because some nitridation processes require a longer time than the milliseconds pulse-modulation cycle. Fig. 10 shows the time-averaged radiation intensity of the nitrogen atomic line as a function of SCL for Q_{N_2}=4.0 slpm. Apparently, the time-averaged radiation intensity increases with decreasing SCL, which indicates

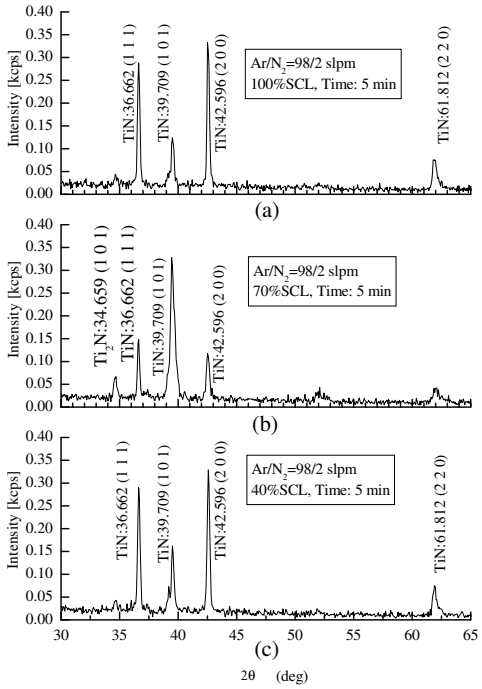

Fig. 8. XRD spectra for specimen surface irradiated by Ar-N_2 PMITP with different shimmer current level [21] [22].

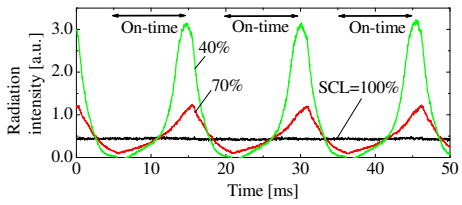

Fig. 9. Time evolutions in the radiation intensity of the nitrogen atomic line at 746 nm from Ar-N_2 PMITP [21] [22].

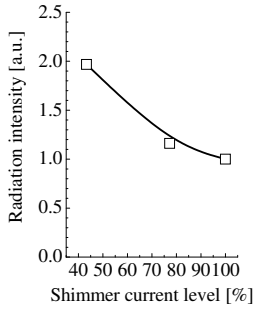

Fig. 10. Time-averaged radiation intensity of the nitrogen atomic line at 746 nm from Ar-N_2 PMITP [21] [22].

that the time-averaged nitrogen density.

For another on-time condition, we found such a more nitrogen excited atom in time-averaged value in modulation operation compared with that in non-modulation operation [23]. Fig. 11 shows the time-averaged radiation intensity of the nitrogen atomic line at 746 nm, being compared with the intensity in non-modulation operation for different on-times. Input power on the horizontal axis in this figure was changed only by changing only on-time. As seen in this figure, we can see a higher intensity at 15–22 kW in modulation operation than that in non-modulation operation.

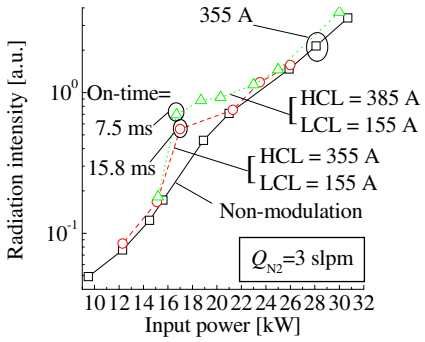

Fig. 11. Time-averaged radiation intensity of the nitrogen atomic line at 746 nm from Ar-N_2 PMITP for different on-time. Input power is changed by changing on-time [23].

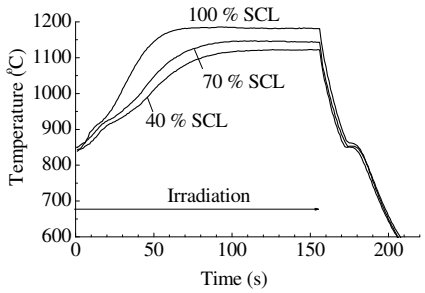

Fig. 12. Temperature variation in surface of specimen irradiated by Ar-N_2 PMITP.

4.4 Modulation effect on the decreased specimen surface temperature The specimen's surface temperature is also principal factor for nitridation and while for thermal damage. Fig. 12 depicts the time variation in the surface temperature of titanium specimens for different SCL cases. The Ar-N_2 PMITP was irradiated from t=0 s in this figure. After irradiation of the Ar-N_2 PMITP, the surface temperature increases with time. The surface temperature is almost saturated at about 100 s after irradiation. The irradiation of the Ar-N_2 PMITP was stopped at t =150 s. After irradiation of the Ar-N_2 PMITP, the surface temperature decreases rapidly with time. It is noteworthy that the surface temperature variation depends on the SCL, although the input power to the inverter power supply is the same value of 15 kW for all cases. From simple analysis of energy balance equation for specimen , it is found that the net enthalpy flow on the specimen was decreased by reduction of SCL [22].

Reducing SCL increases the excited nitrogen atomic density at the same time, as described in the previous section. Consequently, reducing SCL, i.e. the modulation of the coil-current simultaneously causes both an increase in the excited nitrogen atomic density and a decrease in the net enthalpy flow.

4.5 Numerical simulation considering non-equilibrium effects The above phenomena including the increased nitrogen excited atoms and the decreased enthalpy flow that simultaneously obtained

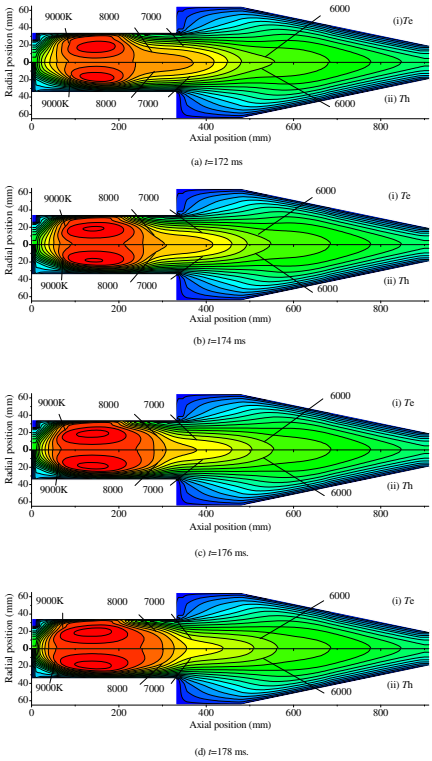

Fig. 13. Transient distribution in electron temperature T_e and heavy particle temperature T_h in Ar-N_2 PMITP.

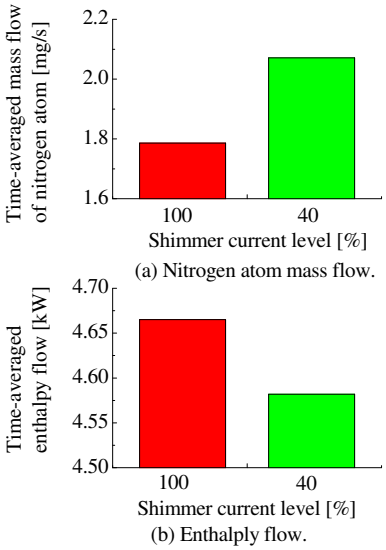

Fig. 14. Temperature variation in surface of specimen irradiated by Ar-N_2 PMITP.

could not be obtained by analysis on the basis of the local thermodynamic equilibrium condition, because more nitrogen excited atoms are obtained by increasing temperature. To confirm this phenomena, we developed a two-dimensional two-temperature chemically non-equilibrium (2D-2T-NCE) model of the Ar-N_2 PMITP [24]–[26]. This model solves a set of mass conservation equations of a bulk plasma, momentum conservation equations, an energy conservation equation for electrons, an energy conservation equation for heavy particles, a mass conservation equation of each species, and a Maxwell equation for the vector potential with a help of the equation of state and the equation of charge neutrality.

Fig. 13 shows the time evolution in spatial distribution of electron temperature T_e and heavy particle temperature T_h in Ar-N_2 PMITP after a rapid increase in coil current from LCL to HCL. The shimmer current level is 40% and Ar/N_2 gas flow rate is 98/2 slpm. In the reaction chamber, T_e is close to T_h. However, in the plasma torch, especially near the torch wall, T_e is apparently more rapidly increased than T_h. This means that pulse modulation of the coil current enhances thermally non-equilibrium effects near the torch wall.

Fig. 14 (a) shows the calculated time-averaged mass flow of nitrogen atom from the Ar-N_2 PMITP into the specimen position by decreasing SCL. The nitrogen gas flow rate is 4 slpm. As indicated in this figure, the time-averaged mass flow of nitrogen atom increases with decreasing SCL from 100% to 40%, meaning that the numerical simulation of Ar-N_2 PMITP also indicates an increase in mass flow of nitrogen atoms onto the specimen surface position. On the other hand, Fig. 14 (b) indicates the calculated time-averaged enthalpy flow from the Ar-N_2 PMITP into the specimen surface position. This figure indicates that a reduction of the SCL from 100% to 40% decreases the time-averaged enthalpy flow. In this way, the numerical simulation also supports the fact that the modulation of the coil current produces such an increase in mass flow of nitrogen atom and a decrease in enthalpy flow simultaneously, which is also obtained in the experiments.

5. Application of Ar-H_2 PMITP to surface modification of specimens

5.1 Application to TiO_2 specimen [18] Ishigaki et al performed an experiment to apply Ar-H_2 PMITP to surface modification of TiO_2. The titanium dioxide (TiO_2) specimen was irradiated by Ar-H_2 PMITP at 26.6 kPa to obtain the effect of PMITP irradiation. The characteristics of TiO_2 strongly depend on the formation of lattice defects and the incorporation of hydrogen.

Fig. 15 shows the XRD spectra from the TiO_2 disk specimen treated in the plasma with and without the coil current modulation at a pressure of 26.6 kPa. The parameter in this figure is the specified position, whose details can be seen in Ref. [18]. As the number of the position parameter in this figure increases from 100 to 200, the distance between the plasma flame and the specimen surface decreases.

As seen in this figure, the phase of all the specimens remains unchanged except for specimen placed in the plasma of continuous mode at a position parameter of 200. However, Fig. 15 (a) indicates that Magneli phases, Ti_nO_{2n-1}, were formed on the surface of the specimen at a position parameter of 200. The disk specimen, treated at position of 200 under 26 kPa in the continous plasma, was directly irradiated by the plasma flame, and then the surface was heated to a temperature higher than the rest of the specimens. As a result, the specimen was

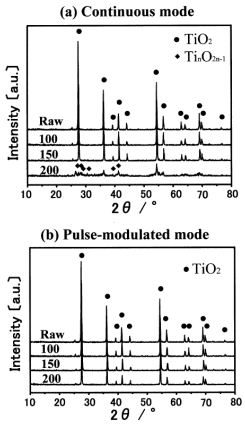

Fig. 15. The XRD spectra from TiO_2 disks placed at various posiitons in Ar-H_2 plasma at a pressure of 26.6 kPa.

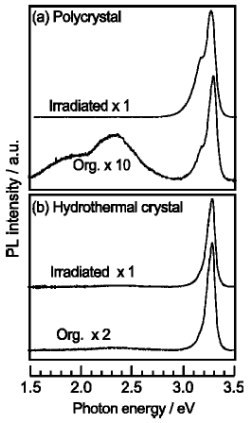

Fig. 16. Typical photoluminescence spectra of ZnO before and after hydrogen plasma irradiation. (a) Polycrystalline ceramic and (b) single crystal grown by the hydrothermal method.

highly reduced from TiO_2 to Ti_nO_{2n-1}.

On the other hand, as represented in Fig. 15 (b), XRD spectra from Magneli phases, Ti_2O_{2n-1}, were not observed. The important point is that the specimens treated in the PMITP were not reduced, even at the highest position of 200, where the specimen temperature is higher that the rest of the samples and the concentration of hydrogen atomis is supposed to be the highest of all three sample positions. Ishigaki et al suggested that this difference in the above results between the irradiation of PMITP and the continuous plasma might be attributed to non-equilibrium effects in the PMITP.

5.2 Application to H doping onto ZnO specimen [19] [20] Here is an example on adoption of PMITP to hydrogen atom doping to ZnO. Many recent investigations on zince oxide (ZnO) have reported about its quantum effect in superlattices, laser emission, and heterojunction light emitting diode. Thus, the control of defects related electron-hole recombination process is important to improve emission efficiency of ZnO. Hydrogen plasma irradiation has been pointed out to be sutable for passivation of ZnO radiative recombination centers giving visible emission (VIS) at 2.3 eV. However, conventional heating technique in a H_2 gas to dope hydrogen atom into ZnO causes the formation of defects such as oxygen vacancy or evaporation of ZnO. Furthermore, ZnO was reduced by continuous irradiation with a non-modulated hydrogen plasma.

Ohashi et al applied Ar-H_2 PMITP for this purpose [19] [20]. Use of the Ar-H_2 PMITP provides less heat accumulation in the irradiation specimen compared with the continuous plasma irradiation. Experimental conditions were as follows: They used on-time of 10 ms, and off-time of 5 ms. The rf frequency was 1 MHz, input power level to a inverter power supply is 13 kW for higher level, while it is 4 kW for lower level. Hydrogen gas flow rate was set to 6×10^{-3} m^3/min, whereas Ar gas flow rate was 98×10^{-3} m^3/min. Total gas pressure was 27 kPa. The irradiation time was 300 s. The details of the experimental setup are available in Ref. [18]

They confirmed in their experiments that Ar-H_2 PMITP irradiation does not reduce ZnO, although a non-modulated plasma irradiation does. In addition, they found the improvement of photoluminescence of ZnO were achieved by irradiation of Ar-H_2 PMITP. Fig. 16 shows the photoluminescence (PL) spectra of ZnO. For original polycrystalline ZnO, there was a broad VIS emission band around 2.3 eV, and an ultraviolet (UV) emission band at 3.3 eV. After irradiation of Ar-H_2 PMITP as indicated in Fig. 16 (a), the VIS emission band disappeared and the UV emission intensity increased by more than ten times. The improvement in UV emission efficiency can be ascribed to the passivation of active centers, which are the origin of the VIS emission.

6. Development of arbitrary waveform modulated induction thermal plasma

6.1 Concept and electric circuit for AMITP Recently, we have developed a new type of modulated induction thermal plasma system, that is, a system of an arbitrary-waveform modulated induction thermal plasma (AMITP) [27]. This system can modulated the coil current sustaining an induction thermal plasma not only into a rectangular waveform but also into an externally-given waveform in milliseconds. Fig. 17 depicts an example of the coil current for AMITP. The coil current amplitude is modulated following an externally-given waveform which is changed in milliseconds.

To realize AMITP, we have developed a new rf power supply which has IGBT and MOSFET elements. Fig. 18 shows the electric circuit for AMITP. The modulation in this case is acheived by switching IGBT. On the other hand, in this power supply, MOSFET elements are switched with a frequency to synchronize a frequency changed by a plasma load with phase-locked loop (PLL) control.

6.2 Dynamic behavior of Ar AMITP Fig. 19 shows (a) the modulation signal, (b) the inverter output current in root-mean-square value, (c) the radiation intensity of the Ar atomic line at 703 nm, and (d) the Ar excitation temperature, in a triangular-rectangular waveform modulation case [27]. Input power is 10 kW,

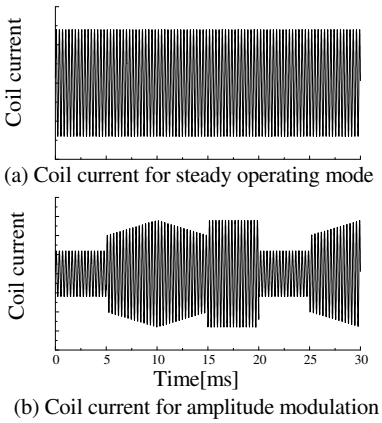

Fig. 17. Coil current for AMITP.

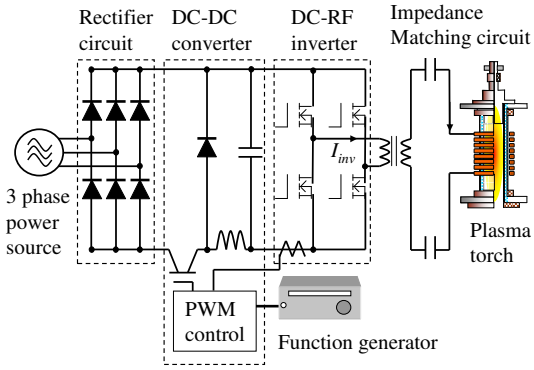

Fig. 18. Electric circuit for AMITP [27].

and the pressure is 5.3 kPa (=40 torr). The observation was carried out at 10 mm below the coil end. The observed radiation intensity changes periodically in triangular waveform according to the modulation control signals with some delay compared to the modulation signal. The delay time was roughly estimated to be 5 ms from the time difference between the minimum of the coil current amplitude and the minimum of the radiation intensity. This delay time in the radiation intensity arises mainly from the thermal inertia of thermal plasmas, which is governed mainly by mass density and specific heat of high temperature Ar gas. Fig. 19 (c) depicts the variation of the radiation intensity for the triangle-rectangular waveform. It is found that the radiation intensity for the rectangular part becomes higher than that for the first triangular part, which is due to the accumulated power input to the plasma.

It is interesting to see how the temperature changes following modulation signal. The Ar excitation temperature was estimated by the two-line method using the two specified Ar lines at 703 and 714 nm. Fig. 19 (d) shows the time evolution in the Ar excitation temperature in case of triangular-rectangular waveform modulation [27]. The Ar excitation temperature is also modulated periodically following a triangular-rectangular control signal, changing from 5500 K to 7000 K. These results implies that the Ar excitation temperature in Ar AMITP can be controlled by the modulated coil current in milliseconds

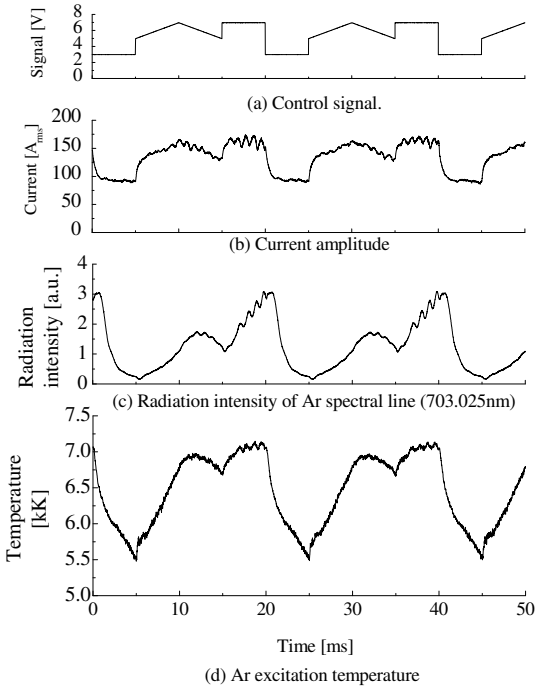

Fig. 19. Time evolution in (a) control signal, (b) modulated coil current, (c) effective power, (d) load resistance, (e) Ar excitation temperature measured in Ar AMITP [27].

in more detailed than that in PMITP.

7. Conclusion

This paper reviews recent results of fundamental dynamic behaviors of PMITPs, and applications of PMITPs. It has been found that the modulation of the coil current can perturb high-pressure high-power thermal plasmas, and can control the temperature and radical densities. Especially Ar excitation temperature in a molecular gas seeded Ar thermal plasma can be changed following the modulated coil current. Application of PMITP to surface modification processing is one of the candidates to utilize chemically non-equilibrium effects ocurring in PMITPs. In addition, a new type of modulated induction thermal plasmas, AMITP has been developed. It was found that more detailed control of the temperature is possible in AMITP than PMITP. The modulated thermal plasma is one promising radical and heat source for high-speed material processings.

References

(1) J.O. Berghaus, J.L. Meunier, and F. Gitzhofer, "Monitoring and control of RF thermal plasma diamond deposition via substrate biasing," *Meas. Sci. Technol.*, **vol. 15**, 161–164, 2004.

(2) S. Matsumoto, M. Hino, and T. Kobayashi, "Synthesis of diamond films in an rf induction thermal plasma," *Appl. Phys. Lett.*, **vol. 51**, 737–739, 1987.

(3) C. Wang, A. Inazaki, T. Shirai, Y. Tanaka, T. Sakuta, H. Takikawa, and H. Matsuo, "Effect of ambient gas and pressure on fullerene synthesis in induction thermal plasma," *Thin Solid Films*, **vol. 425**, 41–48, 2003.

(4) B. Todorovic-Markovic , Z. Markovic, I. Mohai, Z. Karoly, L. Gal, K. Foglein, P.T. Szabo, and J. Szepvolgyi, "Efficient

synthesis of fullerenes in RF thermal plasma reactor," *Chem. Phys. Lett.*, **vol. 378**, 434–439, 2003.
(5) S.L. Girshick, C.P. Chiu, R. Muno, C.Y. Wu, L. Yang, S.K. Singh, and P.H. McMurry, "Thermal plasma synthesis of ultrafine iron particles," *J. Aerosol Sci.*, **vol. 24**, 367–82, 1993.
(6) T. Ishigaki, S.M. Oh, J.G. Li, and D.W. Park, "Controlling the synthesis of TaC nanopowders by injecting liquid precursor into RF induction plasma," *Sci. & Technol. Advanced Mater.*, **vol. 6**, 111–118, 2005.
(7) M. Shigeta, T. Watanabe, and H. Nishiyama, "Numerical investigation for nano-particle synthesis in an RF inductively coupled plasma," *Thin Solid Films*, **vol. 457**, 192–200, 2004.
(8) H. Huang, K. Eguchi, and T. Yoshida, "Novel structured yttria-stabilized zirconia coatings fabricated by hybrid thermal plasma spraying," *Sci. & Technol. Advanced Mater.*, **vol. 4**, 617–622, 2003.
(9) W. R. Chen, X. Wu, B.R. Marple, and P.C. Patnaik, "Oxidation and crack nucleation/growth in an air-plasma-sprayed thermal barrier coating with NiCrAlY bond coat," *Surface & Coatings Technol.*, **vol. 197**, 109–115, 2005.
(10) T. Ishigaki, F. Xiaobao, T. Sakuta, T. Banjo, and Y. Shibuya, "Generation of pulse-modulated induction thermal plasma at atmospheric pressure," *Appl. Phys. Lett.*, **vol. 71**, 3787–3789, 1997.
(11) T. Sakuta, Y. Tanaka, Y. Hashimoto, and M. Katsuki, "Novel system of an inductively coupled thermal plasma with pulse amplitude modulation of electromagnetic field," *Electr. Eng. Japan*, **vol. 138**, 26–33, 2002.
(12) T. Sakuta, Y. Tanaka, K.C. Paul, M.M. Hossain, and T. Ishigaki, "Non-equilibrium effects in pulse modulated induction thermal plasma for advanced processing," *Trans. Mater. Res. Soc. Japan*, **vol. 25**, 35–38, 2000.
(13) Y. Tanaka and T. Sakuta, "Measurement of dynamic response time in pulse modulated thermal plasma," *Trans. Mater. Res. Soc. Japan*, **vol. 25**, 293–296, 2000.
(14) M. M. Hossain, Y. Tanaka, and T. Sakuta, "Transient nature of argon and molecular gas-seeded argon inductive thermal plasmas in pulse amplitude modulation approach," *Trans. IEE of Japan*, **vol. 123-PE**, 1333–1349, 2003.
(15) M. M. Hossain, Y. Tanaka, and T. Sakuta, "Dynamic responses of Ar-CO_2 and Ar-N_2 induction thermal plasmas in pulse modulation approach: a numerical analysis," *Thin Solid Films*, **vol. 435**, 19–26, 2003.
(16) Y. Tanaka and T. Sakuta, "Stable operation region and dynamic behavior of pulse modulated Ar thermal plasma with different molecular gases," *Electr. Eng. Japan*, **vol. 143**, 1–11, 2003.
(17) Y. Tanaka and T. Sakuta, "Temperature control of Ar induction thermal plasma with diatomic molecular gases by pulse-amplitude modulation of coil-current," *Plasma Sources Sci. & Technol.*, **vol. 12**, 69–77, 2003.
(18) T. Ishigaki, H. Haneda, N. Okada, S. Ito, "Surface modification of titanium oxide in pulse-modulated induction thermal plasma", *Thin Solid Films*, **390**, 20–25, 2001.
(19) N. Ohashi, T. Ishigaki, N. Okada, T. Sekiguchi, I. Sakaguchi, and H. Haneda, "Effect of hydrogen doping on ultraviolet emission spectra of various types of ZnO," *Appl. Phys. Lett.*, **vol. 80**, 2869–2871, 2002.
(20) N. Ohashi, T. Ishigaki, N. Okada, H. Taguchi, I. Sakaguchi, S. Hishita, T. Sekiguchi, and H. Haneda, "Passivation of active recombination centers in ZnO by hydrogen doping," *J. Appl. Phys.*, **vol. 93**, 6386–6392, 2003.
(21) Y. Tanaka, T. Muroya, K. Hayashi, and Y. Uesugi, "Simultaneous control of numerical enhancement of N atom and decrease in heat flux into reaction chamber using Ar-N_2 pulse-modulated induction thermal plasmas," *Appl. Phys. Lett.*, **vol. 89**, no. 3, 031501, 2006.
(22) Y.Tanaka, T.Muroya, K.Hayashi, Y.Uesugi, "Control of nitrogen atomic density and enthalpy flow into reaction chamber in Ar-N2 pulse-modulated induction thermal plasmas," *IEEE Trans. Plasma Sci.*, **35**, 197-203, 2007.
(23) Y.Tanaka, K.Hayashi, T.Nakamura, Y.Uesugi, "Influence of ontime on increased number density of excited nitrogen atom in pulse modulated induction thermal plasmas," *J.Phys.D: Appl. Phys.*, **41**, 185203, 2008.
(24) Y. Tanaka and T. Sakuta, "Time-dependent two-dimensional chemical non-equilibrium modeling of Ar-N_2 pulse-modulated induction thermal plasma at atmospheric pressure for material processing," *Trans. Mater. Res. Soc. Japan*, **vol. 29**, 3403–3406, 2004.
(25) Y. Tanaka, "Two-temperature chemically non-equilibrium modelling of high-power Ar-N_2 inductively coupled plasma at atmospheric pressure," *J. Phys. D: Appl. Phys.*, **vol. 37**, 1190–1205, 2004.
(26) Y. Tanaka, "Time-dependent two-temperature chemically non-equilibrium modelling of high-power Ar-N_2 pulse-modulated inductively coupled plasmas at atmospheric pressure," *J. Phys. D: Appl. Phys.*, **vol. 39**, 307–319, 2006.
(27) Y.Tanaka, Y.Morishita, K.Okunaga, S.Fushie, Y.Uesugi, "Generation of high-power arbitrary-waveform modulated inductively coupled plasmas for materials processing," *Appl. Phys. Lett.*, **90**, 071502, 2007.

Yasunori Tanaka (Member) received B.S., M.S., and Ph.D. degrees in electrical engineering from Nagoya University, Japan, in 1993, 1995 and 1998, respectively. In April 1998, he was appointed a Research Associate at Kanazawa University, Japan. He has been working as an Associate Professor since August 2002 at that university. One of his papers has been selected as a leading paper in Journal of Physics D: Applied Physics in 2004. His research interests include arc interruption phenomena and thermal plasma applications. He is a member of IEE of Japan, and a member of Plasma and Fusion Research.

Yoshihiko Uesugi (Member) was born in Japan in 1955. He received a B.E., M.E. and D.E. degrees from Nagoya University in 1977, 1979 and 1983, respectively. After working as a research staff of Japan Atomic Energy Research Institute and an Associate professor of Nagoya University. Now, he is presently a professor of Kanazawa University. His research interests are high power plasma generation and application, and magnetic fusion experiments. He is a member of IEE of Japan and the Japan Society of Plasma Sci. & Nuclear Fusion Research.